

Role of oxygen in $\text{PrBa}_2\text{Cu}_3\text{O}_{7-y}$: Effect on structural and physical properties

M. E. López-Morales,* D. Ríos-Jara, J. Tagüeña, and R. Escudero
*Instituto de Investigaciones en Materiales, Universidad Nacional Autónoma de México,
 Apartado Postal 70-360, México, Distrito Federal, México*

S. La Placa

Thomas J. Watson Research Center, Post Office Box 218, Yorktown Heights, New York 10598-0218

A. Bezinge,† V. Y. Lee, E. M. Engler, and P. M. Grant
IBM Research Division, Almaden Research Center, 650 Harry Road, San Jose, California 95120-6099
 (Received 14 July 1989)

$\text{PrBa}_2\text{Cu}_3\text{O}_{7-y}$ is the only homomorphic member of the entire rare-earth 1:2:3 family which is insulating and not metallic or superconducting. With this unusual behavior in mind, and with an eye to resolving certain questions regarding the widely held notion of otherwise mobile holes held captive in a supravaleant Pr ionic state as its cause, we examined the effect of varying oxygen concentration on the structural, electrical, and magnetic properties of this compound. Powder x-ray diffraction studies revealed an orthorhombic-to-tetragonal order-disorder transition at oxygen levels close to those found for the superconducting lanthanide compounds. From Rietveld-refined powder-neutron-diffraction data taken on a fully oxygenated sample, key insights into the ambivalent character of Pr valency were obtained. Other aspects of Pr valency and carrier dynamics were uncovered by electrical and magnetic measurements as a function of y . We found that the room-temperature resistivity increases by about three orders of magnitude from $y \approx 0$ to $y \approx 0.5$, while the temperature dependence of the paramagnetic susceptibility remains quantitatively the same. We conclude from these results that removal of oxygen from $\text{PrBa}_2\text{Cu}_3\text{O}_{7-y}$ does not substantially alter the valence state of Pr, which we assert to be nominally $3+$, but with strong overlap of its outer-lying $4f$ orbital with neighboring oxygen $2p$ levels results in a characteristically mixed or fluctuating valence situation reminiscent of heavy-fermion systems, and the principal effect on transport properties is on carrier concentration in the chains and steric hindrance of their motion by the resulting oxygen vacancies.

I. INTRODUCTION

Often in the study of superconductivity, understanding the circumstances under which the phenomenon does not occur can be as important to the total picture as understanding those situations when it does. This point becomes especially pertinent when investigating the presence or absence of superconductivity in compounds closely related or identical in structure. Very early in the history of the recently discovered high-temperature superconductors,¹ various rare-earth substitutions for lanthanum in alkaline-earth-doped $\text{La}_2\text{CuO}_{4-y}$ were tried. These attempts were, without exception, unsuccessful in producing new superconductors, as it proved not possible to preserve the underlying K_2NiF_4 crystal structure.² However, the closely related $\text{Nd}_2\text{CuO}_{4-y}$ structure which did form has been recently found to host superconductivity when doped with cerium or thorium.^{3,4} In the case of the prototype $(90+)\text{-K}$ superconductor, $\text{YBa}_2\text{Cu}_3\text{O}_{7-y}$, all rare-earth elements, save three, when substituted for yttrium yielded superconductors in roughly the same 90-K range,⁵ even though most of these lanthanide ions possessed spin magnetic moments, normally a condition extremely unfavorable for supercon-

ductivity. The three exceptions were Ce, Tb, and Pr. It was found that Ce and Tb do not form the "1:2:3" phase⁶ and so naturally would not be expected to behave as the others. On the other hand, Pr does substitute directly for Y yielding $\text{PrBa}_2\text{Cu}_3\text{O}_{7-y}$, yet it does not superconduct. It is the only such example in the entire set of lanthanide compounds isomorphic to $\text{YBa}_2\text{Cu}_3\text{O}_{7-y}$. In fact, it is an insulator.

On the surface, this result is quite perplexing, as Pr 1:2:3 shares with its fellow rare-earth 1:2:3 compounds a number of features thought necessary for high-temperature superconductivity, such as the presence of CuO planes and a high concentration of oxygen in its unit cell ($y \approx 0$) when prepared appropriately. At one time it was widely thought that an orthorhombic structure was a necessary condition for superconductivity in all high- T_c materials and some early work indicated that $\text{PrBa}_2\text{Cu}_3\text{O}_{7-y}$ might be tetragonal at $y = 0$.⁷⁻⁹ However, it is now known that Pr 1:2:3 is indeed orthorhombic,¹⁰ and, in any event, the discovery of the layered bismuth and thallium compounds proved that tetragonal superconductors can exist.¹¹

A possible explanation for the lack of superconductivity (and normal-state metallic behavior) in $\text{PrBa}_2\text{Cu}_3\text{O}_{7-y}$

can be found in the knowledge that mixed valent oxides of Pr exist, e.g., Pr_6O_{11} ($\text{Pr}^{3,7+}$) and PrO_2 (Pr^{4+}).¹² Therefore, if Pr were indeed in a 4+ state, then no excess positive charge above the nominal ionic values of its other constituents (Ba^{2+} , Cu^{2+} , and O^{2-}) would be present in stoichiometric $\text{PrBa}_2\text{Cu}_3\text{O}_{7-y}$ with $y=0$ to support metallic conduction and superconductivity. However, it can be quickly seen that this picture is far too simple. A number of groups^{7,13,14} have studied the solid solution system $\text{Y}_{1-x}\text{Pr}_x\text{Ba}_2\text{Cu}_3\text{O}_{7-y}$ and found T_c to decrease monotonically with increasing Pr concentration, disappearing completely for $x > 0.5-0.6$, whereas, on the above mixed valent argument, this should not have occurred until $x=1$ (assuming $y \approx 0$). Various explanations can be constructed as to why superconductivity was quenched at lower Pr concentrations than might have been expected. On the assumption that Pr is 4+, the condition for unit cell charge neutrality in $\text{Y}_{1-x}\text{Pr}_x\text{Ba}_2\text{Cu}_3\text{O}_{7-y}$ is $x + 3\delta + 2y - 1 = 0$ where δ is the amount of excess charge relative to Cu^{2+} . If the Y,Pr solid solutions were oxygen deficient in the amount $y=0.2$, then a Pr concentration $x=0.6$ would suffice to reduce δ to zero. It could also be argued that a critical carrier concentration is necessary to support superconductivity, as in the $\text{La}_2\text{CuO}_{4-y}$ compounds, so that one might expect the suppression of superconductivity for at some value $x < 1$. Moreover, it is possible the extra charge is disproportionated among the CuO planes and chains in the 1:2:3 unit cell, and that the introduction of Pr^{4+} affects only the charge in that part of the network responsible for superconductivity resulting in $T_c \rightarrow 0$ for $x < 1$. Finally, it has been suggested¹⁵ that the dependence of T_c on x can be modeled on the Abrikosov-Gorkov (AG) theory¹⁶ of pair breaking by paramagnetic impurities, in this case moments on the lattice of Pr ions.

Core level spectroscopy measurements have been made^{17,18} in an effort to determine the Pr charge state in $\text{PrBa}_2\text{Cu}_3\text{O}_{7-y}$. The shape and position of the observed Pr absorption edge strongly point to Pr^{3+} . Recent constant initial state photoemission measurements by Kang *et al.*¹⁹ also suggest a Pr^{3+} core state. Raman studies undertaken with similar hopes of ascertaining the Pr valence state have also been performed, but with mixed results. Rosen *et al.*²⁰ find no significant departure of the $\text{PrBa}_2\text{Cu}_3\text{O}_{7-y}$ Raman spectrum from the other lanthanide 1:2:3 systems and thus conclude Pr is trivalent, whereas Thomsen *et al.*²¹ on the basis of almost similar data, but with slightly lower Cu-O vibrational frequencies, support a Pr^{4+} interpretation.

With all these issues in mind, we undertook to study the effect of oxygen concentration on the structural and physical properties of $\text{PrBa}_2\text{Cu}_3\text{O}_{7-y}$, paying particular attention to the question of Pr valency and the possible influence of y on its value. In Sec. II we discuss our synthetic approach, focusing on those special conditions for the preparation of impurity-free material and its characterization. Section III contains the results of our

TABLE I. Summary of iodometric titration results for $\text{PrBa}_2\text{Cu}_3\text{O}_{7-y}$: unit cell oxygen content, $7-y$, and total excess charge per unit cell, p . Data from this table, in conjunction with powder diffraction measurements, were used to construct Fig. 2.

Sample	$7-y$	p
A3 ^a	6.46	-0.033
A2	6.54	0.027
A1	6.56	0.042
B ^a	6.60	0.067
A	6.61	0.073
B2	6.84	0.227
B1	6.85	0.233
C2	6.86	0.240
B3	6.88	0.253
B4 ^a	6.93	0.287
C1	6.96	0.306
IV92C ^b	6.96	0.310

^aSamples used for transport and magnetic measurements.

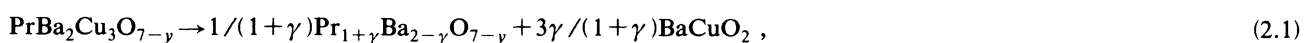
^bSample for neutron powder diffraction.

powder-neutron-diffraction studies on fully oxygenated $\text{PrBa}_2\text{Cu}_3\text{O}_{7-y}$ and the implications for Pr valency. Resistivity, susceptibility, and thermopower data as a function of oxygen concentration are examined in Sec. IV. Finally, in Sec. V we discuss our results against the background of measurements and models of other workers.

II. SYNTHESIS AND CHARACTERIZATION

Samples were prepared by standard solid state reaction techniques. Appropriate molar quantities of Pr_6O_{11} , BaCO_3 , and CuO were mixed and reacted in an alumina crucible at 900 °C for a minimum of 24 h in air. The resultant product was then reground with a mortar and pestle, pressed into pellets, and recalined at 950 °C for at least 14 d, with no less than 5 intermediate grindings. The samples were quenched (<5 min) to room temperature from the final heating stage. The oxygen concentration at this point was typically 6.6 atoms per unit cell. Selected samples were then annealed in flowing oxygen at 500 °C for various periods of time to increase their oxygen content. For example, sample B 4 (see Table I) was treated in this manner for 120 min resulting in 6.93 oxygen atoms per unit cell. On the other hand, some samples (e.g., A1, A2, and A3) were annealed in vacuum at 600 °C to further lower their oxygen level from the original quenched state.

The above preparative procedure parallels that used for the other lanthanide 1:2:3 systems. However, we have found important differences stand out for the synthesis of Pr compounds. Some workers^{8,22} have held that phase separation governed by the following equation,



is inevitable in Pr 1:2:3 reactions. However, we believe Eq. (2.1) merely represents an incomplete reaction. We found that with sufficiently high temperatures and long enough calcining times, we could obtain a complete reaction without the presence of secondary phases. This can clearly be seen in Fig. 1 where the number and intensity of secondary phase powder x-ray diffraction lines (mostly due to BaCuO_2 as above and also various Pr suboxides) is shown to decrease with longer processing time. It can take as long as three weeks to obtain a sample whose x-ray spectrum is free from these secondary phases, an indication that the diffusion of Pr in these solid state reactions is extremely slow.

Thermogravimetric analyses were also performed on several of the samples. Fully oxygenated specimens were heated in flowing nitrogen gas at a rate of $10^\circ\text{C}/\text{min}$. A two step weight loss, denoting evolution of oxygen from the sample, was observed beginning at 400°C and continuing to approximately 600°C , with a secondary decrease starting at 700°C on up to 900°C at which temperature the oxygen content per unit cell as estimated from total weight loss was roughly six. The higher temperature weight drop starting at 700°C has been associated with the orthorhombic-tetragonal transition in other 1:2:3 compounds.²³ Thus, the thermodynamics and kinetics of oxygen stability and transport in $\text{PrBa}_2\text{Cu}_3\text{O}_{7-y}$ seem not to be substantially different from those of yttrium 1:2:3;²³ that is, oxygen insertion and removal in $\text{PrBa}_2\text{Cu}_3\text{O}_{7-y}$ occurs only in the interbarium CuO chains as in $\text{YBa}_2\text{CuO}_3\text{O}_{7-y}$.

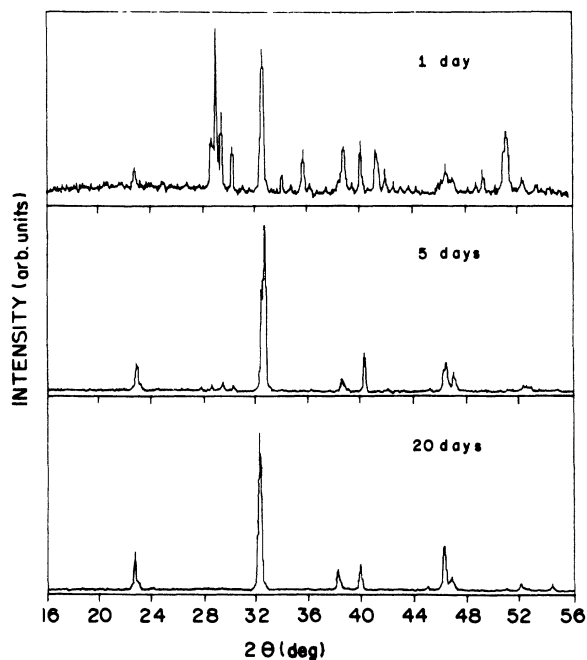


FIG. 1. Comparison of the powder x-ray diffraction patterns with length of reaction time indicating the importance of multiple regrinding and recalcining operations for $\text{PrBa}_2\text{Cu}_3\text{O}_{7-y}$. Note the complete disappearance of secondary phases after 20 d.

Sample oxygen content was quantitatively determined by an iodometric titration technique following the procedure described by Nazzari *et al.*²⁴ This method, which involves two separate titrations, when applied to most lanthanide copper oxide compounds can uniquely determine the amount of extra positive charge associated with the copper-oxygen bond and, in addition, the total number of oxygen atoms per unit cell. However, in the case of Pr 1:2:3, and other compounds where particular cation valencies may be uncertain, the technique must be applied with caution. Because in acidic solutions Pr^{4+} and $[\text{CuO}]^+$ are equally reduced to Pr^{3+} and $[\text{CuO}]$, respectively, it is not possible in the absence of additional data to uniquely apportion the measured excess positive charge between these two complexes. On the other hand, one can still assess the total oxygen content under the assumption of proper cation stoichiometry. Table I summarizes our results for samples subsequently used for structural, transport, and magnetic measurements. The excess positive charge per unit cell, p , calculated from the titration data under the assumption that the Ba and O charge states are nominally $2+$ and $2-$, respectively, is given in the second column. However, as pointed out above, the distribution of charge between the Pr and Cu cationic complexes cannot be uniquely determined from titration alone. We thus defer further discussion of this point to the appropriate sections to follow.

III. STRUCTURAL ASPECTS

The structural properties as a function of oxygen content were measured by powder x-ray diffraction. Samples were ground and mixed with dehydrated NaCl which was used to simultaneously calibrate interplane distances. An automated diffraction, utilizing CuK_α radiation and a secondary powder monochromator, was used to obtain the requisite spectra, and standard indexing techniques applied to derive unit cell parameters. The dependence of the unit cell dimensions on oxygen concentration²⁵ ranging from $6.97 > 7-y > 6.15$ (see Table I) is shown in Fig. 2. As in the superconducting yttrium homologue, we observe an orthorhombic-to-tetragonal transition when $7-y$ passes below roughly 6.6. That this transition can occur in a totally insulating 1:2:3 single phase compound as well as in its superconducting isomorphs suggests the metal-insulator transition accompanying the structural transition in the conducting 1:2:3 materials merely signals the onset of long-range oxygen disorder on the scale of detectability by normal powder diffraction methods. That is, the orthorhombic-to-tetragonal transition as a function of oxygen concentration is an order-disorder effect and is not associated with an electronic instability in any of the 1:2:3 compounds. We note in passing that the degree of orthorhombicity, as gauged by the ratio $(b-a)/(b+a)$, of $\text{PrBa}_2\text{Cu}_3\text{O}_{7-y}$ (0.0084) is less than that of $\text{YBa}_2\text{Cu}_3\text{O}_{7-y}$ (0.0092),²⁶ but larger than that of the rest of the lanthanide series, and also that the orthorhombic-tetragonal transition occurs at a slightly higher oxygen concentration than in the yttrium compound. This latter fact may be due to the lower degree of

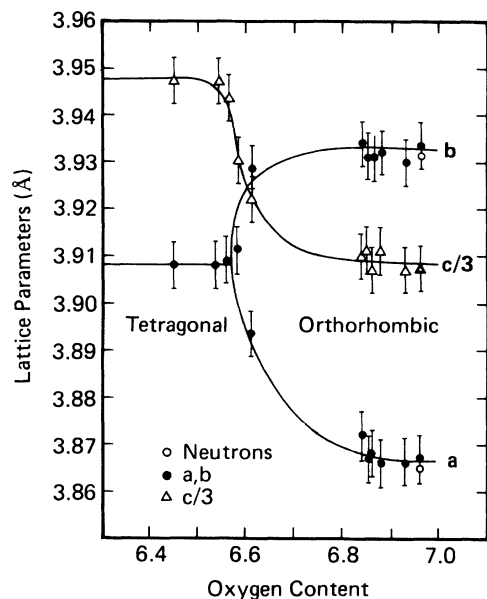


FIG. 2. Unit cell lattice parameters of $\text{PrBa}_2\text{Cu}_3\text{O}_{7-y}$ as a function of oxygen content $7-y$, as determined by powder x-ray diffraction. Also displayed are the powder-neutron-diffraction values near $y=0$. The c parameters found by x-rays and neutrons overlap as shown. Note the onset of an orthorhombic-tetragonal transition as the oxygen content drops below $7-y \approx 6.6$.

orthorhombicity in $\text{PrBa}_2\text{Cu}_3\text{O}_{7-y}$ and consequently an earlier onset of average tetragonality is seen in powder x-ray diffraction.

We now draw attention to the variation in c -axis parameter with oxygen concentration as given in Fig. 2. At first sight, it might seem attractive to correlate the expansion observed as oxygen is removed to a Pr^{4+} - Pr^{3+} ionic transition, and, indeed, the increase in c that is obtained would correspond to about half the distance expected from the difference in respective ionic radii. However, as will be seen, our magnetic data indicate that little change in Pr ionic state occurs as oxygen is withdrawn. Moreover, essentially the same c -parameter expansion, including the jump in the region $6.4 < 7-y < 6.7$, was found²⁷ in $\text{YBa}_2\text{Cu}_3\text{O}_{7-y}$ as $y \rightarrow 1$. In $\text{YBa}_2\text{Cu}_3\text{O}_{7-y}$, the change in c is associated with an enlargement of the planar copper to apical oxygen [Cu(2)-O(1)] distance, and it is quite likely this is the case for $\text{PrBa}_2\text{Cu}_3\text{O}_{7-y}$ as well, and thus not connected to any change in Pr-O bond distance and thus in Pr ionic state. The observation of such similar oxygen-dependent behavior in the c axis of nonsuperconducting $\text{PrBa}_2\text{Cu}_3\text{O}_{7-y}$ may require a reinterpretation of the $\text{YBa}_2\text{Cu}_3\text{O}_{7-y}$ anomalies as reflecting charge redistribution within the 1:2:3 unit cell. It may be that the c -axis expansion is due primarily to local ion rearrangement when enough negative charge is removed from the chains, and the "jump" near $y=0.5$ might be a sign of the twofold superlattice ideally formed at this concentration.

Powder-neutron-diffraction measurements were performed on sample IV92C (see Table I). These room-

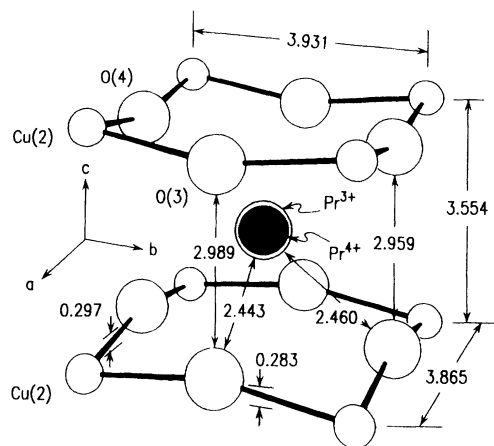


FIG. 3. Central portion of the unit cell of $\text{PrBa}_2\text{Cu}_3\text{O}_{7-y}$ as determined by powder neutron diffraction. The figure shows the planar Cu-O "cage" surrounding the Pr ion. Pr-O bond distances, as well as the Cu-O deviations from planarity, are between the centers of the designated atoms. All length units are in Å. The diameters of the Pr, Cu, and O ions are drawn relative to their respective ionic radii in the appropriate coordination, with their absolute values reduced by $\frac{1}{3}$ from the scale of the rest of the figure for clarity.

temperature data were collected at the Brookhaven High Flux Beam Reactor facility under conditions similar to those described by Cox *et al.*²⁸ and a subsequent structure refinement carried out using the Rietveld technique.²⁹ From the refinement, the oxygen content of sample IV92C was determined to be very nearly seven per unit cell, in close agreement with the titration data from Table I. The cell symmetry was found to be orthorhombic (space group $Pmmm$) with lattice parameters $a=3.8654(2)$, $b=3.9309(2)$, and $c=11.7250(7)$ Å, respectively. As seen from Fig. 2, these values fall within the error bars of the x-ray values for this sample.

We now discuss some of the structural characteristics of $\text{PrBa}_2\text{Cu}_3\text{O}_{7-y}$ as revealed by the neutron results, with the hope of deducing a clue to the ionic character of Pr. Figure 3 shows atomic positions in the Pr 1:2:3 unit cell and the labeling conventions which will subsequently be used. Table II summarizes the interatomic bond distances between Pr-O, Cu-O, and Cu-Cu, while Table

TABLE II. Interatomic distances as determined by powder neutron diffraction. See Fig. 3 for positional notation.

Atomic pair	Distance (Å)
Pr-O3	2.443
Pr-O4	2.460
Cu(1)-O1	1.965
Cu(1)-O2	1.854
Cu(2)-O2	2.232
Cu(2)-O3	1.989
Cu(2)-O4	1.955
Cu(1)-Cu(2)	4.086
Cu(2)-Cu(2)	3.554

III contains the atom positions in normalized orthorhombic cell coordinates. These data can be analyzed in at least two separate ways in an attempt to determine the Pr charge state: (1) by examining the separation between CuO planes surrounding the Pr cation (the "slot" width), or (2) the average Pr—O bond distances and comparing both quantities against similar values for the rest of the lanthanide series and generally accepted values for the ionic radii of trivalent rare earths in eightfold coordination.³⁰ Application of the first method is summarized in Table IV, and in Fig. 4 (left-hand axis), expanding on an earlier analysis of similar data by Le Page *et al.*³¹ The results of the second method, contained in Table V and also in Fig. 4 (right-hand axis), are obtained using the mean Pr—O bond length in combination with other lanthanide-oxygen distances in the rare-earth 1:2:3 compounds. The excellent correlation of measured lanthanide 1:2:3 slot widths with corresponding trivalent ionic radii shown in Fig. 4 employing approach (1) presents a compelling argument that Pr is indeed also trivalent in PrBa₂Cu₃O_{7-y}. Any other value, even slightly departing from Pr³⁺, would cause Pr 1:2:3 to fall significantly outside the otherwise smooth dependence of slot width on rare-earth ionic radius displayed by the rest of the lanthanide 1:2:3 compounds. On the other hand, application of method (2) suggests that Pr in fact cannot be trivalent. We see from Table V that the mean Pr—O bond length, taken as the average of Pr—O(3)(2.440 Å) and Pr—O(4)(2.460 Å), is much too short for Pr³⁺O²⁻ with Pr and O in coordinates eight and four, respectively. We show this in Table V in terms of an effective oxygen radius significantly less than expected for that of O²⁻ in a fourfold environment. We see that analyzing the R—O distances in this way for other rare-earth (Ho, Y, and Gd) 1:2:3 compounds where sufficient data exist does indeed lead to effective oxygen ionic radii consistent with O²⁻. For the case of La 1:2:3, we must take into account that, in this compound, the Ba—O and Cu—O bond distances are close to the La—O distances (due to the large radius of La³⁺), thus making oxygen sixfold coordinated instead of fourfold. When this is done, the value found for the effective O²⁻ radius contained in Table V agrees well

TABLE III. Atomic positions of PrBa₂Cu₃O₇ with respect to orthorhombic unit cell coordinates [$a=3.8654(2)$ Å, $b=3.9309(2)$ Å, and $c=11.7250(7)$ Å], as determined by powder neutron diffraction.

Atom	x	y	z
Pr	0.5	0.5	0.5
Ba	0.5	0.5	0.188 ^a
Cu(1)	0.0	0.0	0.0
Cu(2)	0.0	0.0	0.3485
O1	0.0	0.5	0.0
O2	0.0	0.0	0.1581
O3	0.0	0.5	0.3726
O4	0.5	0.0	0.3739

^aThis value was estimated from the structure for YBa₂Cu₃O_{6.74} as given in Ref. 26, Kajitani *et al.* Jpn. J. Appl. Phys. **26**, L1144 (1987).

TABLE IV. Comparison of the Cu(2)—Cu(2) interplanar, or "slot," distance d_{slot} , with source referenced, with increasing trivalent state ionic radii R_R for various rare-earth elements R in RBa₂Cu₃O₇. Values of ionic radii are from Ref. 30. Data from this table were used in constructing Fig. 4. Distance units are in Å.

R	d_{slot}	Ref.	R_R
Er	3.350	a	1.144
Ho	3.367	b	1.155
Y	3.369	c	1.159
Gd	3.395	d	1.193
Nd	3.513	a	1.249
Pr	3.554	This work	1.266
La	3.676	e	1.30

^aS. J. La Placa, unpublished data.

^bReference 6.

^cReference 26.

^dJ. A. Campá, J. M. Gómez de Salazar, E. Gutiérrez-Puebla, M. A. Monge, I. Rasines, and C. Ruíz-Valero, Phys. Rev. B **37**, 529 (1988).

^eM. Izumi, K. Uchinokura, A. Maeda, and S. Tanaka, Jpn. J. Appl. Phys. **26**, L1555 (1987).

with standard values for O²⁻ in coordination six.³⁰ The uniqueness of the Pr—O bond distance in PrBa₂Cu₃O_{7-y} compared to the other lanthanide 1:2:3 systems is shown in that part of Fig. 4 where we plot measured R—O bond

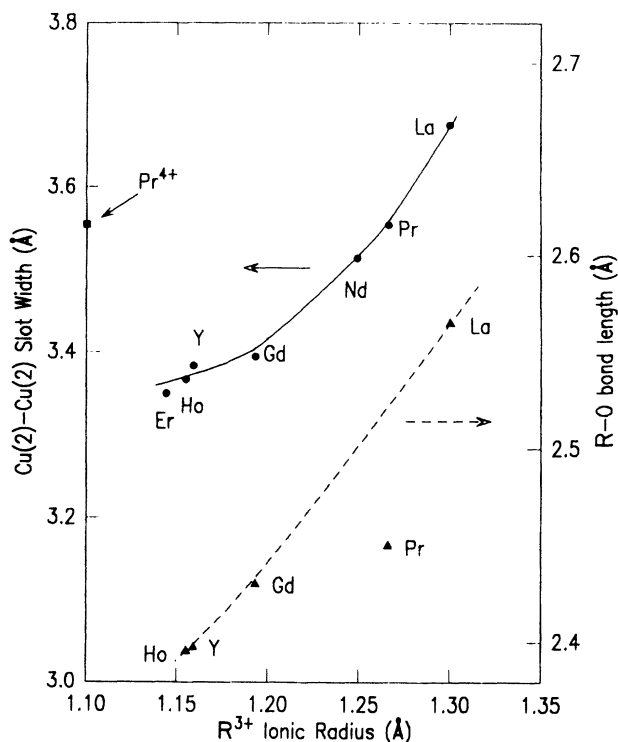


FIG. 4. Experimental values of the Cu(2)—Cu(2) slot distances and R—O bond lengths as a function of trivalent R ionic radii. The slot distance for PrBa₂Cu₃O_{7-y} positioned at the ionic radius of Pr⁴⁺ is shown for comparison against the overwhelmingly experimental 3+ trend of the entire R series. Lines through the data are for the purpose of guiding the eye.

TABLE V. Mean ionic radii, $\langle R_{\text{Oxygen}} \rangle$, of the O3 and O4 atoms in several rare-earth 1:2:3 compounds, as deduced from the mean rare-earth–oxygen–bond length, $\langle d_{R-O} \rangle$, contained in the referenced structural data, compared with the trivalent state ionic radii R_R in eightfold coordination for various rare-earth elements R in $\text{RBa}_2\text{Cu}_3\text{O}_7$. Values of ionic radii are from Ref. 30. Data from this table were used in constructing Fig. 4. See text for methodology and discussion. Distance units are in Å.

R	$\langle d_{R-O} \rangle$	Ref.	R_R	$\langle R_{\text{Oxygen}} \rangle$
Ho	2.395	a	1.155	1.240
Y	2.397	b	1.159	1.238
Gd	2.430	c	1.193	1.237
Pr	2.451	this work	1.266	1.184
La	2.565	d	1.30	1.265

^aReference 6.

^bReference 26.

^cJ. A. Campá, J. M. Gómez de Salazar, E. Gutiérrez-Puebla, M. A. Monge, I. Rasines, and C. Ruíz-Valero, *Phys. Rev. B* **37**, 529 (1988).

^dM. Izumi, K. Uchinokura, A. Maeda, and S. Tanaka, *Jpn. J. Appl. Phys.* **26**, L1555 (1987).

lengths against trivalent R ionic radii. We see that the neutron value for $\text{PrBa}_2\text{Cu}_3\text{O}_{7-y}$ is much smaller than the trend found for the other R^{3+} 1:2:3 compounds. If we simply interpolate the measured Pr—O distance between those expected for octahedrally coordinated $\text{Pr}^{3+}\text{O}^{2-}$ and $\text{Pr}^{4+}\text{O}^{2-}$ complexes,³⁰ we obtain an effective Pr charge of $+3.4$.

How, then, do we reconcile these two seemingly different conclusions the structural data yield concerning the ionic state of praseodymium in $\text{PrBa}_2\text{Cu}_3\text{O}_{7-y}$? That is, why does the slot distance strongly point to Pr^{3+} , while a direct examination of the Pr—O bond length suggests a more nearly tetravalent state? The answer becomes clear when we consider that the slot distance in 1:2:3 compounds is determined by the hard sphere contact between the R ion and its surrounding Cu^{2+} cage. However, the short Pr—O bond distance, and its attendant strong warping of the surrounding Cu—O planes, tells us that considerable hybridization is occurring which spreads charge out into the oxygen bond. Nevertheless, this negative charge remains inside the Cu^{2+} cage. Thus, the total charge confined within this cage is still $3+$ effectively yielding a Pr^{3+} ionic radius which sets the slot distance. This picture provides an explanation of the Raman results, which do not directly probe the R —O bond, but rely inferentially on changes in the $\text{Cu}(2)$ -O(3,4) bending frequencies as a function of R ionic radius to determine its charge state. Rosen *et al.*²⁰ show that the position of this frequency is consistent with a trivalent ionic radius throughout the entire lanthanide series, including praseodymium. This finding is in accord with our argument above that the size of the surrounding CuO cage is set by the total enclosed charge of $3+$. For single crystal $\text{PrBa}_2\text{Cu}_3\text{O}_{7-y}$, Thomsen *et al.*,¹² who favor an interpretation in terms of Pr^{4+} for essentially similar data, find a 9-cm^{-1} difference in the position of this mode from Rosen *et al.*²⁰ which they attribute to the formation

of Pr^{3+} in the latter's samples due to possible oxygen deficiency. Actually, the crystal of Thomsen *et al.*²¹ had tetragonal symmetry, which, on the basis of the data in Fig. 2, would indicate their sample to be oxygen deficient. However, as will be seen, it is a moot point since our magnetization measurements show little or no change in Pr valency as a function of oxygen concentration.

Our structural analysis thus solves the paradox as to why certain data, e.g., core level spectra, seemingly require Pr to be trivalent, while other experiments, such as the dependence of T_c on x in $\text{Y}_{1-x}\text{Pr}_x\text{Ba}_2\text{Cu}_3\text{O}_{7-y}$, point to $4+$. We will elaborate more in Sec. V.

IV. PHYSICAL PROPERTIES

The temperature dependence of the resistivity, thermopower, and magnetic susceptibility was measured at three oxygen concentrations from the sample set contained in Table I: $7-y=6.93$, 6.60 , and 6.46 (B4, B, and A3). The results are shown in Figs. 5–8.

The resistivity data were taken by a standard low-frequency ac technique monitoring both phase shift and contact resistance as a function of temperature.³² Silver paste contacts were painted around the sample and lock-in detection with current densities kept less than $10 \mu\text{A}/\text{cm}^2$. The sample itself was cemented directly onto a Lake Shore diode (calibrated to ± 0.5 K) with GE varnish assuring that both the thermometer and sample were in equilibrium at all temperatures. The resistivity shows a qualitatively similar insulating temperature dependence at all three concentrations; however, we were unable to fit the data very well to any of the usual transport models for such behavior. No single activation energy gap could be found,³³ nor were we able to obtain fits to the usual

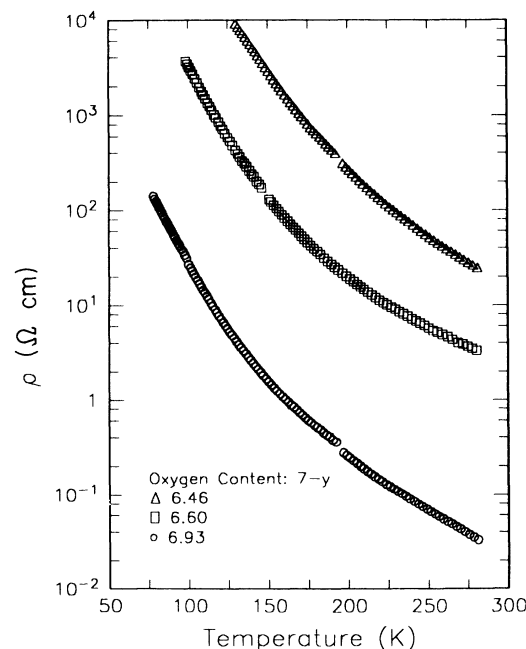


FIG. 5. Temperature dependence of the resistivity of $\text{PrBa}_2\text{Cu}_3\text{O}_{7-y}$ as a function of $7-y$ for three selected samples.

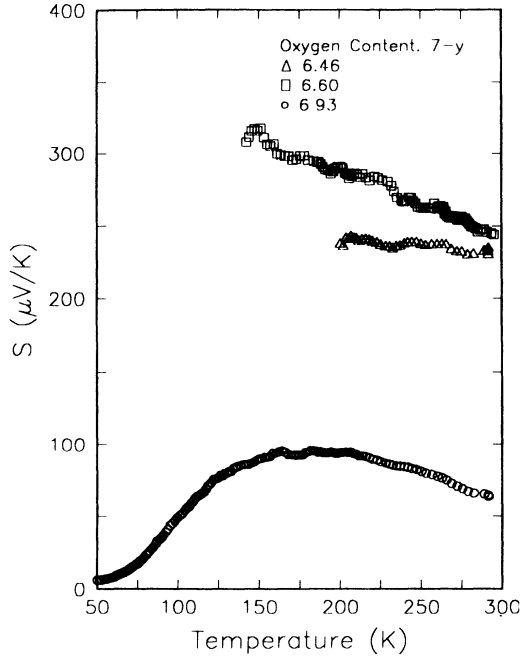


FIG. 6. Temperature dependence of the thermopower of $\text{PrBa}_2\text{Cu}_3\text{O}_{7-y}$ as a function of $7-y$ for three selected samples. The magnitude of S for the $7-y=6.46$ sample (Δ) is depressed from its true value due to the high sample resistance with respect to the input impedance of the null detectors used in our thermopower apparatus.

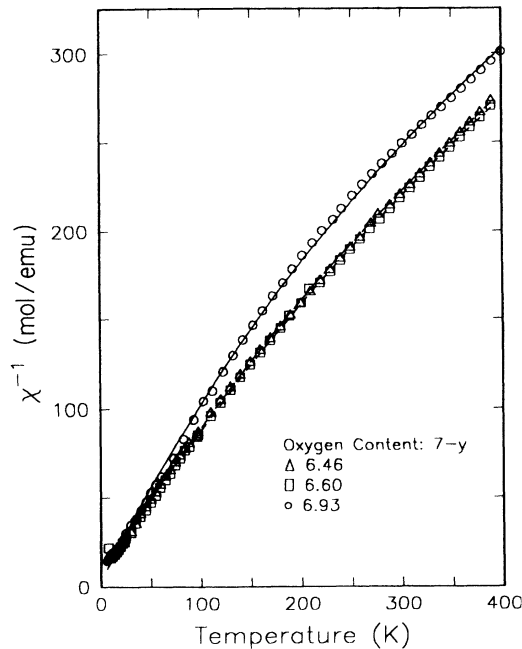


FIG. 7. Temperature dependence of the inverse susceptibility of $\text{PrBa}_2\text{Cu}_3\text{O}_{7-y}$ as a function of $7-y$ for three selected samples. The solid lines represent fits of the data to a Curie-Weiss law of the form $\chi = \chi_0 + C/(T + \Theta)$, from which the effective Pr charge state is subsequently estimated. The parameter values yielded by the fits are summarized in Table VI.

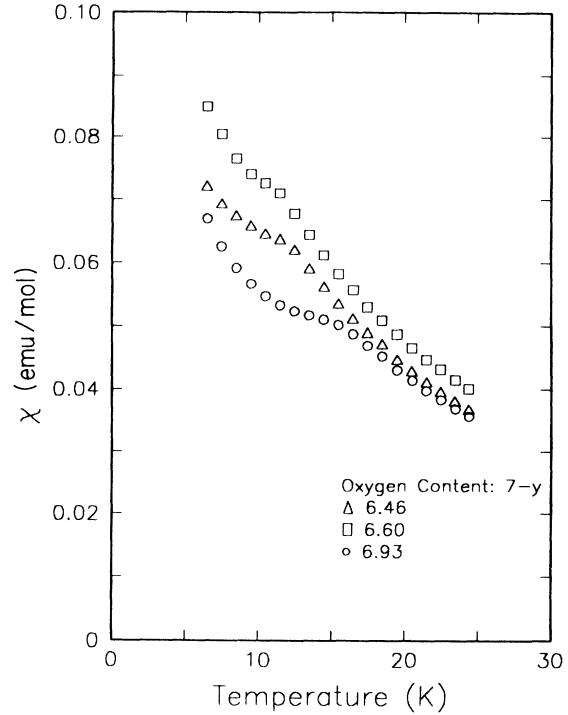


FIG. 8. The susceptibility of $\text{PrBa}_2\text{Cu}_3\text{O}_{7-y}$ at low temperature as a function of $7-y$ for three selected samples. Note the onset of a magnetic transition in the region 14–17 K.

formulas for variable range hopping in one, two, or three dimensions.³⁴ We also see from Fig. 5 that ρ increases by more than three orders of magnitude at all temperatures as the oxygen content is reduced. One explanation is that near $y=0$, a small number of holes may indeed exist that are capable of electrical conduction, and that this number perhaps decreases somewhat as oxygen is taken out.

Support for this picture is given by the changes observed in thermopower as indicated in Fig. 6 which shows the magnitude of S at room temperature to more than double as $7-y$ goes from 6.93 to 6.46, a typical indication that the number of carriers has been reduced. However, we must point out that the almost three orders of magnitude increases in resistivity at all temperatures on removal of approximately 0.5 oxygen atoms per unit cell cannot be explained by changes in carrier concentration alone. We will have more to say about this in the Discussion. The thermopower measurements were performed using an apparatus similar to that described by Chaikin and Kwak.³⁵ Samples of rectangular dimension of the order of a few tenths of a millimeter with a length to width ratio of 5:1 or higher were secured from pressed pellets. These samples were attached to 10-mil gold wires with silver paste. The gold wires served as both electrical and thermal contacts. Differential temperature across the gold-sample series network was measured with an iron-gold-chromel thermocouple. Due to the very high sample electrical resistances, we were not able to obtain thermopower data at very low temperatures, especially for the deoxygenated samples, in our apparatus.

TABLE VI. Curie-Weiss parameters, χ_0 , Θ , and C , as determined by fitting the data of Fig. 7 with $\chi = \chi_0 + C/(T + \Theta)$, followed by the effective Bohr magneton, $\mu^* = (3kC/\mu_B^2)^{1/2}$, and the effective Pr charge, $Q_{Pr} = 3 + (\mu_{3+}^* - \mu^*)/(\mu_{3+}^* - \mu_{4+}^*)$, where $\mu_{3+}^* = 3.62$ and $\mu_{4+}^* = 2.54$ for the two respective Pr valence states. $p_{[CuO]}$ is the average excess charge per CuO unit. See text for methodology and discussion.

Sample	$7-y$	Θ (K)	χ_0 (emu/mol)	C (emu K/mol)	μ^*	Q_{Pr}	$p_{[CuO]}$
B4	6.93	3	11×10^{-4}	0.9	2.7	3.8	0.02
B	6.60	7	9×10^{-4}	1.1	2.9	3.7	-0.17
A3	6.46	8	9×10^{-4}	1.1	2.9	3.7	-0.26

In contrast to ρ and S , the inverse magnetic susceptibility, χ^{-1} , shown in Fig. 7, does not exhibit a marked dependence of oxygen content. Our magnetometry measurements were performed using a SHE Corporation Series 900 variable temperature SQUID susceptometer in an applied field of 0.1 T. Since the observed paramagnetism in $\text{PrBa}_2\text{Cu}_3\text{O}_{7-y}$ arises almost totally from the spin state of the Pr ion (the contribution from Cu 2+ is about 100 times less), the implication is that the charge state of Pr is not much affected by the withdrawal of oxygen from the chains. This is reinforced by the Curie-Weiss fits denoted by the solid curves in Fig. 7, and summarized in Table VI, which yielded values for the effective Bohr magneton clustered in the narrow range 2.7 to 2.9. Figure 8 contains the low-temperature behavior of the susceptibility. In all three samples, we see evidence of the magnetic transition observed by Jee *et al.*,³⁶ and also found in specific heat,³⁷ suppressed slightly by 3–4 K on removal of oxygen, but still occurring at an extraordinarily high temperature, another indication that the chain oxygen occupation has only a small effect on the state of the Pr ion or its surrounding CuO planes.

V. DISCUSSION

We will first discuss the results of the magnetic measurements. It turns out the magnetic properties of $\text{PrBa}_2\text{Cu}_3\text{O}_{7-y}$ have several features in common with other praseodymium oxides. For example, a departure from simple linear Curie-like behavior of $1/\chi$ versus T in PrO_2 was observed some time ago by Kern³⁸ and others.³⁹ A fit of the high-temperature data to a Curie-Weiss law [$\chi = C/(T + \Theta)$, see Table VI caption] yielded, as was the case for our data, a quite small effective Bohr magneton, μ_B^* , of the order 2.5. Moreover, these workers also observed a magnetic anomaly at roughly 14 K which was interpreted by MacChesney *et al.*³⁹ as the onset of antiferromagnetism. In a later paper, Kern *et al.*,⁴⁰ using inelastic neutron scattering, confirmed this interpretation, obtaining an ordered Pr moment of approximately $0.6\mu_B$. Recently, Li *et al.*,⁴¹ also using neutron techniques, found similar results for $\text{PrBa}_2\text{Cu}_3\text{O}_{7-y}$; i.e., a Néel temperature $T_N = 17$ K and an effective Pr moment equal to $0.24\mu_B$ [$(0.74 \pm 0.08)\mu_B$ for $T \ll T_N$]. In retrospect, given the magnetic behavior of PrO_2 , the results for $\text{PrBa}_2\text{Cu}_3\text{O}_{7-y}$ could have been anticipated. The small differences in T_N and respective paramagnetic and anti-

ferromagnetic μ_B^* between the two materials might possibly arise from the tetrahedral coordination of Pr in the former compared to octahedral in the latter.

Since the nominal ionicity of Pr in PrO_2 is 4+, it is tempting to conclude, in view of its similar magnetic behavior, that Pr in $\text{PrBa}_2\text{Cu}_3\text{O}_{7-y}$ is also in nearly the same state. A Pr charge state significantly higher than 3+ which is invariant to oxygen content, as compared to the strong dependence of the transport properties, implies that whatever carriers are available for conduction in this material must reside in the chains rather than the planes. Otherwise, one might expect metallic behavior and superconductivity near $y=0$ (attempts by us to synthesize $\text{PrBa}_2\text{Cu}_3\text{O}_{7-y}$ with $y < 0$ by annealing under high oxygen pressure have not proved successful). The most elementary approach to explaining the difference between $\text{PrBa}_2\text{Cu}_3\text{O}_{7-y}$ and its superconducting homologues is to take the analysis in Table VI literally; that is, that the effective Pr charge, Q_{Pr} , is given simply by a linear interpolation within bounding Pr^{3+} and Pr^{4+} magnetic moments. The average charge per CuO unit, $p_{[CuO]}$, shown in the right-most column of Table VI, is given by the charge neutrality relation, $Q_{Pr} + 4 + 3(2 + p_{[CuO]}) - 2(7 - y) = 0$. Theoretical⁴² and experimental⁴³ evidence indicates removal of oxygen in 1:2:3 compounds first depletes the CuO plane hole population until it reaches zero, with subsequent oxygen reduction affecting carrier concentration in the chains. Tokura *et al.*⁴³ argue that the extra positive charge per unit cell in $\text{YBa}_2\text{Cu}_3\text{O}_{7-y}$, $y=0$, is distributed equally between the two CuO planes and the single CuO chain. Thus, at $y=0.5$, all holes are removed from the planes, thereby suppressing metallic behavior and superconductivity, leaving 0.5 holes in the chain which remain localized. For $\text{PrBa}_2\text{Cu}_3\text{O}_{7-y}$, this picture implies that $Q_{Pr} = 3.5$ has the same effect as $y=0.5$; that is, complete removal of itinerant holes from the CuO planes. This same argument would also explain why superconductivity in $\text{Y}_{1-x}\text{Pr}_x\text{Ba}_2\text{Cu}_3\text{O}_{7-y}$ disappears at $x \approx 0.5$ providing $Q_{Pr} = 4.0$. Therefore, for $Q_{Pr} > 3.5$, all remaining charge resides in the chain, and the average charge $p_{[CuO]}$ should be tripled to give chain charge carrier concentrations 0.06, -0.5, and -0.72 for the three samples shown.

However, this view, namely that of a nearly tetravalent Pr which localizes permanently all itinerant plane holes, is most likely very oversimplified. If such a description actually held on a sufficiently long time scale, the resultant charge localization should have been revealed in the

spectroscopic and structural results. As pointed out in Sec. I, various core level spectroscopy observations strongly indicate that Pr is trivalent in PrBa₂Cu₃O_{7-x}.^{17,18} We also mentioned that the Raman²⁰ data and CuO interplane slot distances suggest Pr³⁺. Finally, the relatively small effective moments obtained from the Curie-Weiss fits most likely result from strong crystalline electric fields arising from the Pr-O hybridization which quench a nominally Pr³⁺ moment, thus mimicking Pr⁴⁺ and calling into question interpretations to this end that might possibly be drawn from Table VI. The main lesson taught by the magnetic data of Figs. 7 and 8 and the analysis given in Table VI is that nothing much happens to the central Cu-Pr-O cage on removal of oxygen from PrBa₂Cu₃O_{7-y}.

A more appropriate electronic model for PrBa₂Cu₃O_{7-y} is suggested by the results of our structural study set forth in Sec. III. There we concluded that, although the total integrated charge within the central cage is consistent with Pr³⁺, as given by the cage dimensions, the short Pr—O bond length indicates considerable hybridization of the outerlying Pr orbitals with O 2*p* states. Strong supporting evidence for such a model can also be found in recent resonant photoemission (RESPES) data obtained by Kang *et al.*¹⁹ on Y_{1-x}Pr_xBa₂Cu₃O_{7-y} solid solutions. They observed, at all finite values of *x*, a large 4*f* electron density only 1 eV below the hole Fermi level pinned near the top of the oxygen 2*p* band. On the other hand, the constant initial state photoemission from these 4*f* levels has the same spectral dependence as the 4*f* state in Pr metal, where Pr is commonly assumed to be 3+. These data, along with our structural findings, indicate that we must be careful not to strictly equate valency with ionicity when discussing the electronic state of Pr in PrBa₂Cu₃O_{7-y}. In fact, the spectroscopic results on PrBa₂Cu₃O_{7-y} are typical of those generally found in other mixed valent Pr, Ce, and Tb oxides.⁴⁴ Indeed, the magnetic measurements themselves, especially the very high Néel temperature, suggest strong mixing of the Pr 4*f* states with O 2*p* orbitals, not only in PrBa₂Cu₃O_{7-y}, but in most other Pr oxides as well.⁴⁵ The idea that such mixed, or fluctuating, valence states, may supply a means for understanding PrBa₂Cu₃O_{7-y}, has been put forward by several groups.^{36,13,46}

We therefore suggest the following lattice Anderson Hamiltonian⁴⁷⁻⁴⁹ as the framework most suitable for discussing the electronic properties of not only PrBa₂Cu₃O_{7-y} but the entire rare-earth 1:2:3 family as well:

$$\mathcal{H} = \mathcal{H}_{\{R\}} + \mathcal{H}_{\{CuO_2\}} + \mathcal{H}_{\{R\},\{CuO_2\}}. \quad (5.1)$$

Here we have partitioned the total Hamiltonian into an *R* sublattice term, a term treating only the CuO₂ planes and then an interaction term between these two systems. Explicitly, each of these terms are as follows:

$$\mathcal{H}_{\{R\}} = \sum_{i\alpha} \epsilon_{i\alpha}^f f_{i\alpha}^\dagger f_{i\alpha} + \sum_{i\alpha\beta\gamma\delta} U_{\alpha\beta\gamma\delta} f_{i\alpha}^\dagger f_{i\beta}^\dagger f_{i\gamma} f_{i\delta}, \quad (5.2)$$

where *i* indexes the *R* sites, α, \dots, δ index the degenerate states, including spin, of the *R* 4*f* shell, $\epsilon_{i\alpha}^f$ is the position

of these states with respect to the Fermi energy of the planar CuO₂ holes, and $U_{\alpha\beta\gamma\delta}$ the Coulomb repulsion within and between these same states. $f_{i\alpha}^\dagger$ and $f_{i\alpha}$ are the appropriate fermion operators for the *R* 4*f* manifold. Essentially, the above expression is a zero-bandwidth degenerate Hubbard Hamiltonian. Next, for the CuO₂ planes, we have

$$\begin{aligned} \mathcal{H}_{\{CuO_2\}} = & \sum_{j \neq j', \sigma} [t_{jj'}(1 - n_{j, -\sigma}) d_{j\sigma}^\dagger d_{j'\sigma}(1 - n_{j', -\sigma})] \\ & + J \sum_j \mathbf{S}_j \cdot \mathbf{S}_{j+1}, \end{aligned} \quad (5.3)$$

where *j, j'* are the Cu site indices, σ the spin index of the CuO peroxide hole, d_j^\dagger , d_j , and n_j its fermion and occupation operators, respectively, $t_{jj'}$ the effective hole hopping integral, *J* the nearest neighbor antiferromagnetic exchange integral between Cu²⁺ sites, and \mathbf{S}_j the spin- $\frac{1}{2}$ operator on each of these sites. $\mathcal{H}_{\{CuO_2\}}$ is the effective one-band Hamiltonian (the “*t*-*J*” model) derived by Rice and Zhang⁵⁰ from the two-band Hubbard model for planar CuO₂ in the small bandwidth limit. The third term in Eq. (5.1) represents the single particle interaction between the lanthanide and CuO₂ sublattices and is of the usual form for the Anderson impurity model:

$$\mathcal{H}_{\{R\},\{CuO_2\}} = \sum_{ij\alpha(\sigma)} [V_{ij}^\alpha f_{i\alpha(\sigma)} d_{j\sigma} + \text{H.c.}] \quad (5.4)$$

In this term, V_{ij}^α is the spin-conserving interaction, or hybridization, parameter which takes an electron from the localized *R* 4*f* levels to annihilate the planar CuO₂ hole and vice versa. This term is characteristic of many mixed valence, fluctuating valence, and heavy fermion models, except that here, instead of the usual pair of creation-annihilation operators, two annihilation operators appear due to our choice of a hole representation for the itinerant carriers. For PrBa₂Cu₃O_{7-y}, RESPES indicates ϵ^f to be small and our measured Pr—O bond length points to large *V*, conditions ideal for fluctuating valence. Figure 9 contains a simplified schematic representation of Eqs. (5.1)–(5.4) in the context of the PrBa₂Cu₃O_{7-y}, 4*f* manifold. The probability of trapping a hole in the lanthanide 4*f* state could be extremely large, and we emphasize this model must hold for the entire *R* 1:2:3 system.⁵¹ It is beyond the scope of this paper to pursue a detailed analysis of Eqs. (5.1)–(5.4), but clearly the relative magnitudes of ϵ^f and *V* with respect to *t*, *U*, and *J* will dominate that part of the parameter phase diagram which separates superconducting from insulating behavior in the lanthanide 1:2:3 systems. This phase boundary has to be crossed on moving from Nd 1:2:3 to Pr 1:2:3, and, in fact, it appears to be crossed in Y_{1-x}Pr_xBa₂Cu₃O_{7-y}, *x*=0.5, at around 10 kbar of hydrostatic pressure,¹³ where a metal-insulator transition is observed, a consequence of inherent decreases in ϵ^f and increases in *V* under pressure relative to the other parameters in Eqs. (5.1)–(5.4). In PrBa₂Cu₃O_{7-y}, the time scale for carrier localization must be short enough that major structural rearrangements cannot take place, yet at the same time be long enough to prevent not only pair formation, but normal metallic conductivity as well. Equations

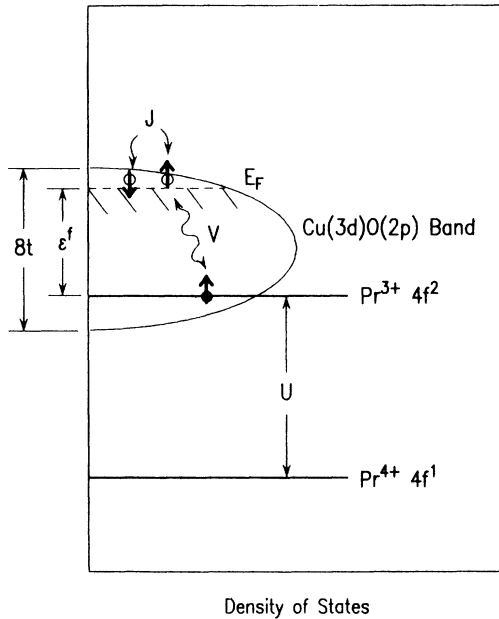


FIG. 9. Simplified schematic representation of energies and interaction terms in Eqs. (5.1)–(5.4). For clarity, we have tacitly assumed V weak enough that a single particle picture can be drawn near E_F .

(5.1)–(5.4) also contain the necessary ingredients for Pr-Pr magnetic coupling via Ruderman-Kittel-Kasuya-Yoshida (RKKY) or superexchange interactions. As pointed out by Li *et al.*,⁴¹ the high value of the Néel temperature in $\text{PrBa}_2\text{Cu}_3\text{O}_{7-y}$, and PrO_2 for that matter, would rule against RKKY coupling, and, in any event, these materials are insulating and lack a Fermi liquid state to mediate such an interaction. It is more likely that the high T_N arises from an enhanced superexchange coupling enabled by the strong Pr 4f–O 2p hybridization. As an alternative to carrier localization, Kebede *et al.*¹⁵ have proposed that this interaction results in AG pair breaking which then becomes the mechanism suppressing superconductivity in $\text{Y}_{1-x}\text{Pr}_x\text{Ba}_2\text{Cu}_3\text{O}_{7-y}$. However, although quite novel and intriguing, we believe this idea has some inherent difficulties. Firstly, paramagnetic pair breaking in classical low- T_c superconductors does not normally lead to destruction of the metallic state at impurity concentration levels where $T_c = 0$. Secondly, one would not expect to see marked increases in room-temperature resistivity as paramagnetic impurities are introduced. Different workers disagree as to what is actually observed with increasing x in $\text{Y}_{1-x}\text{Pr}_x\text{Ba}_2\text{Cu}_3\text{O}_{7-y}$. Kebede *et al.*¹⁵ found ρ (100 K) to be essentially independent of x for $0 < x < 0.5$, whereas Gonçalves *et al.*⁵² see an increase in ρ (300 K) of about five times that for $x=0$ over the same Pr concentration range. More recent results by the Temple-Tufts collaboration⁵³ are in closer agreement with the room-temperature data of the latter. A simple carrier concentration model, based on the assumption of a 4+ state for Pr, would be given by $\sigma = \sigma_c + (1-x)\sigma_p^0$, where σ_c and σ_p^0 are the chain and plane conductivities,

respectively, the latter defined for $x=0$. Since $\sigma_p^0 \gg \sigma_c$, the actual increase in ρ at small x could be difficult to observe given the inevitable vagaries in sample preparation and densities. On the other hand, it might be thought that AG pair breaking by the Pr magnetic moment in the “ n -type” $\text{Pr}_{2-x}\text{Ce}_x\text{CuO}_{4-y}$ high- T_c compound,³ where the Pr ion occupies a similar lattice position relative to the CuO plane as it does in $\text{PrBa}_2\text{Cu}_3\text{O}_{7-y}$. However, no magnetic ordering of the Pr moments is observed⁵⁴ above 1.5 K in the parent compound $\text{Pr}_2\text{CuO}_{4-y}$, indicating hybridization with oxygens in the CuO plane is far less than in Pr 1:2:3. Presumably, this is because Pr in the former compound has additional oxygen coordination apart from the CuO plane oxygens. Also, one would not expect Eqs. (5.1)–(5.4), which apply explicitly to holes, to hold for the n -type superconductors.

We now discuss the temperature and oxygen concentration dependence of the resistivity in $\text{PrBa}_2\text{Cu}_3\text{O}_{7-y}$ as shown in Fig. 5. Two unusual aspects are apparent—both previously brought up in Sec. IV. The first is the lack of agreement in the temperature dependence with any of the usual models for activated or variable range hopping transport. The second striking feature is the extremely strong increase in resistivity at all temperatures on oxygen withdrawal, far greater than one would expect from changes in carrier concentration, although some shift of carriers from the high-mobility planes to low-mobility chains cannot be ruled out entirely. We believe it is more likely that this second feature arises from steric hindrance of thermally activated carrier transport by removal of the bridging oxygen along the b axis in the interbarium plane of the 1:2:3 unit cell. Figure 10 simulates transport in this plane through use of a two-

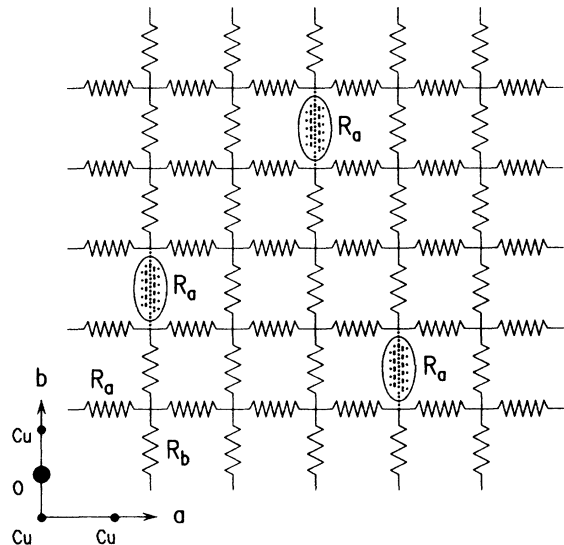


FIG. 10. Two-dimensional resistor lattice model for transport in the interbarium plane of $\text{PrBa}_2\text{Cu}_3\text{O}_{7-y}$. R_a and R_b denote conduction along the oxygen-vacant and oxygen-containing unit cell directions a and b , respectively. Shown schematically are three random oxygen-vacant positions along the chain resulting in the replacement of R_b by R_a .

dimensional resistor network, R_a representing current flow along the oxygen vacant direction, and R_b that in the oxygen bridging direction, with $R_a \gg R_b$. Removal of an oxygen atom would result in effectively replacing R_b by R_a at that particular position. A wide range of bulk resistivity dependence on oxygen concentration can be obtained depending on whether removal occurs randomly or in stages. For example, assuming that at $y=0.25$ all oxygen had been removed from every other chain, one might expect the resistivity to simply double, whereas a random distribution of vacancies would result in a much larger increase. We are currently testing various configuration scenarios for the Fig. 10 network by computer simulation. Recent results for $\text{YBa}_2\text{Cu}_3\text{O}_{7-y}$ by Beyers *et al.*⁵⁵ indicate that a complex set of superlattice structures form as oxygen is removed from the interbarium plane under equilibrium conditions. In principle, we would expect the same behavior for $\text{PrBa}_2\text{Cu}_3\text{O}_{7-y}$ as a function of y , given the very similar aspects of its Thermogravimetric Analysis (TGA) relative to $\text{YBa}_2\text{Cu}_3\text{O}_{7-y}$. However, our samples were not quenched and annealed under the same equilibrium conditions as the Y 1:2:3 study, and we suspect that our oxygen vacancies are much more randomly distributed thus leading to the large changes in resistivity observed in Fig. 5. We are undertaking a more detailed investigation of the normal-state transport as a function of y in $\text{PrBa}_2\text{Cu}_3\text{O}_{7-y}$. Unlike $\text{YBa}_2\text{Cu}_3\text{O}_{7-y}$, where the plane conductivity shorts out that in the chain, $\text{PrBa}_2\text{Cu}_3\text{O}_{7-y}$ provides an excellent vehicle to isolate and study chain transport specifically.

Lastly, we discuss the thermopower data contained in Fig. 6. The temperature dependence of the $7-y=6.93$ sample is in general agreement with that found by Gonçalves *et al.*,^{52,56,67} displaying a curious decrease in magnitude below 150 K, yet not crossing zero, even though the resistivity continues to increase. This is quite unexpected as S should behave as $1/T$ in the usual model for a semiconductor. Such peculiar behavior might actually be related to the inability to fit ρ versus T to an activated model, suggesting that an energy gap does not exist in the usual sense in $\text{PrBa}_2\text{Cu}_3\text{O}_{7-y}$. The most spectacular speculation about the drop in S would be that it is evidence for superconducting fluctuations that never quite stabilize. However, this drop could also signal a transition to a highly correlated narrow band regime, as suggested by Gonçalves *et al.*, in which the thermopower is governed by the temperature independent model of Chaikin and Beni.⁵⁸ Such behavior would be consistent with the increase in the linear specific heat term with increasing Pr content observed in Y-Pr 1:2:3 solid solutions.⁵³ On the other hand, the decrease in thermopower magnitude might also be a general feature of heavy-fermion-like systems described by Eqs. (5.1)–(5.4). Something like this is indeed seen in the thermopower of mixed-valent cerium materials where a fall in S occasions the onset of a valence instability.⁵⁹ For the moment, the

temperature dependence of the thermopower in $\text{PrBa}_2\text{Cu}_3\text{O}_{7-y}$ remains an enigma, and an indication that charge transport in this material requires a deeper understanding than that provided by a simple model of carrier excitation across a Pr^{4+} - Pr^{3+} gap.

Finally, Fig. 6 shows that as the net unit cell charge becomes negative with respect to Cu^{2+} on removal of oxygen (see Table VI), S nonetheless remains positive and increases in magnitude. This finding argues against the use of an effective mass description in terms of holes and electrons in high- T_c materials, a point made recently in regard to high-temperature superconductors in general.⁶⁰

VI. SUMMARY

In conclusion, we have shown that removing oxygen from $\text{PrBa}_2\text{Cu}_3\text{O}_{7-y}$ results in a number of interesting effects. First of all, Pr 1:2:3 undergoes the same orthorhombic-to-tetragonal order-disorder transition as do its metallic and superconducting isomorphs, thus proving such behavior is not unique to the latter systems. For the full oxygenated case, $y \approx 0$, using powder-neutron-diffraction refinement, we show that the structure manifests features characteristic of both Pr^{3+} and Pr^{4+} , a finding which resolves much of the past confusion and apparently conflicting experimental data on the issue of Pr valency in $\text{PrBa}_2\text{Cu}_3\text{O}_{7-y}$.

In addition, we find that oxygen depletion induces a strong quantitative change of transport properties toward more insulating behavior, with little concomitant effect on magnetic properties. These observations indicate that lowering oxygen concentration has virtually no effect on Pr ionicity, and that its overall impact on transport is to sterically hinder carrier motion in the chains. With respect to the transport and magnetic properties of the planes, we propose a periodic Anderson impurity model as the proper theoretical framework for the entire R 1:2:3 series, suggesting that a metal- and/or superconductor-insulator transition will occur at model parameters appropriate for Pr.

ACKNOWLEDGMENTS

We have benefited from useful conversations with a number of colleagues, both within and without our respective institutes, particularly A. Nazzal, R. B. Beyers, S. S. P. Parkin, and R. M. MacFarlane; and Z.-X. Shen, A. McMahan, J. Jorgensen, J. C. Grow, and J. W. Lynn. J. E. Vazquez performed the transport measurements contained in this paper. We also thank F. Morales and L. Baños for technical assistance. The authors from the Instituto de Investigaciones en Materiales, Universidad Nacional Autónoma de México (IIM-UNAM) gratefully acknowledge financial support from Programa Universitario de Superconductores Ceramicos de Alta Temperatura.

- *Currently on sabbatical leave at the IBM Almaden Research Center, San Jose, California.
- †Present address: Condensed Matter Physics, University of Geneva, Switzerland.
- 1 J. G. Bednorz and K. A. Müller, *Z. Phys. B* **64**, 189 (1986).
 - 2 IBM Almaden Research Center High- T_c Team (unpublished work). At that time, we were unaware of previous Soviet work on these materials (I. S. Shaplygin, B. G. Kakhan, and V. B. Lazerev, *Z. Neorg. Khim.* **24**, 1478 (1979) [*Russ. J. Inorg. Chem.* **24**, 820 (1979)]) which showed that they were not metallic.
 - 3 Y. Tokura, H. Takagi, and S. Uchida, *Nature* **337**, 345 (1989).
 - 4 J. T. Markert and M. B. Maple, *Solid State Commun.* (to be published); J. T. Markert, E. A. Early, T. Bjornholm, S. Ghamaty, B. W. Lee, J. J. Neumeier, R. D. Price, C. L. Seaman, and M. B. Maple, *Physica* **158C**, 178 (1989).
 - 5 E. M. Engler, V. Y. Lee, A. I. Nazzal, R. B. Beyers, G. Lim, P. M. Grant, S. S. P. Parkin, M. L. Ramirez, J. E. Vazquez, and R. J. Savoy, *J. Am. Chem. Soc. Commun.* **109**, 2848 (1987).
 - 6 K. Zhang, Ph.D. thesis, Illinois Institute of Technology, 1988, unpublished.
 - 7 L. Soderholm, K. Zhang, D. G. Hinks, M. A. Beno, J. D. Jorgensen, C. U. Segre, and I. K. Schuller, *Nature* **328**, 604 (1987).
 - 8 K. Kinoshita, A. Matsuda, H. Shibata, T. Ishii, T. Watanabe, and T. Yamada, *Jpn. J. Appl. Phys.* **27**, L1642 (1988).
 - 9 J. K. Liang, X. T. Xu, S. S. Xie, G. H. Rao, X. Y. Shao, and Z. G. Duan, *Z. Phys. B* **69**, 137 (1987).
 - 10 M. E. López-Morales, D. Ríos-Jara, J. Tagüena-Martínez, R. Escudero, and J. Gómez-Lara, *Physica* **153–155C**, 942 (1988).
 - 11 R. B. Beyers and T. M. Shaw, *Solid State Phys.* **42**, 135 (1989).
 - 12 Throughout most of this paper, unless otherwise indicated, the terms valency and ionicity will be used interchangeably.
 - 13 M. B. Maple, Y. Dalichaouch, E. A. Early, B. W. Lee, J. T. Markert, M. W. McElfresh, J. J. Neumeier, C. L. Seaman, M. S. Torikachvili, K. N. Yang, and H. Zhou, in *Proceedings of the International Discussion Meeting on High- T_c Superconductors*, Schloss Mauterndorf, Austria, 1988 (Plenum, New York, to be published).
 - 14 C.-S. Jee, A. Kebede, D. Nichols, J. E. Crow, T. Mihalisin, G. H. Myer, I. Perez, R. E. Salomon, and P. Schlottmann, *Solid State Commun.* **69**, 704 (1989).
 - 15 A. Kebede, C.-S. Jee, D. Nichols, M. V. Kuric, J. E. Crow, R. P. Guertin, T. Mihalisin, G. H. Myer, I. Perez, R. E. Salomon, and P. Schlottmann, *J. Magn. Magn. Mater.* **76–77**, 619 (1988).
 - 16 A. A. Abrikosov and L. P. Gorkov, *Zh. Eksp. Teor. Fiz.* **39**, 1781 (1961) [*Sov. Phys.—JETP* **12**, 1243 (1961)].
 - 17 F. Lytle, R. Greegor, E. Marques, E. Larson, J. Wong, and C. Violet (unpublished).
 - 18 E. E. Alp, G. K. Shenoy, L. Soderholm, G. L. Goodman, D. G. Hinks, B. W. Veal, P. A. Montano, and D. E. Ellis, *Proceedings MRS Symposium on High Temperature Superconductivity*, Boston, 1987, pp. 177–182.
 - 19 J.-S. Kang, J. W. Allen, Z.-X. Shen, W. P. Ellis, J. J. Yeh, B.-W. Lee, M. B. Maple, W. E. Spicer, and I. Landau, *J. Less-Common Met.* **148**, 121 (1989).
 - 20 H. J. Rosen, R. M. Macfarlane, E. M. Engler, V. Y. Lee, and R. D. Jacowitz, *Phys. Rev. B* **38**, 2460 (1988).
 - 21 C. Thomsen, R. Liu, M. Cardona, U. Amador, and E. Moran, *Solid State Commun.* **67**, 271 (1988).
 - 22 B. Okai, M. Kosuge, H. Nozaki, K. Takahashi, and M. Ohta, *Jpn. J. Appl. Phys.* **27**, L41 (1988).
 - 23 P. K. Gallagher, H. M. O'Bryan, S. A. Sunshine, and D. W. Murphy, *Mater. Res. Bull.* **22**, 995 (1987).
 - 24 A. Nazzal, V. Y. Lee, E. M. Engler, R. D. Jacowitz, Y. Tokura, and J. B. Torrance, *Physica* **153–155C**, 1367 (1988); *Mater. Res. Bull.* **22**, 995 (1987).
 - 25 M. E. López-Morales, D. Ríos-Jara, R. Escudero, F. Morales, E. M. Engler, V. Y. Lee, A. Bezingé, S. S. P. Parkin, and P. M. Grant (unpublished).
 - 26 T. Kajitani, K. Oh-ishi, M. Kikuchi, Y. Syono, and M. Hirabayashi, *Jpn. J. Appl. Phys.* **26**, L1144 (1987).
 - 27 R. J. Cava, B. Batlogg, K. M. Rabe, E. A. Rietman, P. K. Gallagher, and L. W. Rupp, *Physica* **156C**, 523 (1988).
 - 28 D. E. Cox, S. C. Moss, R. L. Meng, P. H. Hor, and C. W. Chu, *J. Mater. Res.* **3**, 1327 (1988).
 - 29 L. M. Rietveld, *J. Appl. Crystallogr.* **2**, 65 (1969).
 - 30 R. D. Shannon, *Acta Crystallogr. A* **32**, 751 (1976).
 - 31 Y. Le Page, T. Siegrist, S. A. Sunshine, L. F. Schneemeyer, D. W. Murphy, S. M. Zahurak, J. V. Waszczak, W. R. McKinnon, J. M. Tarascon, G. W. Hull, and L. H. Greene, *Phys. Rev. B* **36**, 3617 (1987).
 - 32 M. L. Ramirez, J. E. Vazquez, and P. M. Grant, IBM Research Report No. RJ6457, available from IBM Almaden Research Center Library.
 - 33 S. Kambe, K. Kishio, N. Ooba, N. Sugii, K. Kitazawa, and K. Fuecki, *Supercond. Mater.*, p. 11 (1988).
 - 34 N. F. Mott and E. A. Davis, *Electronic Processes in Non-crystalline Materials* (Clarendon, Oxford, 1979).
 - 35 P. M. Chaikin and J. F. Kwak, *Rev. Sci. Instrum.* **46**, 218 (1975).
 - 36 C.-S. Jee, A. Kebede, T. Yuen, S. H. Bloom, M. V. Kuric, J. E. Crow, R. P. Guertin, T. Mihalisin, G. H. Myer, and P. Schlottmann, *J. Magn. Magn. Mater.* **76–77**, 617 (1988).
 - 37 H. P. van der Meulen, J. J. M. Franse, Z. Tarnawski, K. Kadowaki, J. C. P. Klasse, and A. A. Menovsky, *Physica* **152C**, 65 (1988).
 - 38 S. Kern, *J. Chem. Phys.* **40**, 208 (1964).
 - 39 J. B. MacChesney, H. J. Williams, R. C. Sherwood, and J. F. Potter, *J. Chem. Phys.* **41**, 3177 (1964).
 - 40 S. Kern, C.-K. Loong, and G. H. Lander, *Phys. Rev. B* **32**, 3051 (1985).
 - 41 W.-H. Li, J. W. Lynn, S. Skanthakumar, T. W. Clinton, A. Kebede, C.-S. Jee, J. E. Crow, and T. Mihalsin, *Phys. Rev. B* **40**, 5300 (1989).
 - 42 Y. Guo, J.-M. Langlois, and W. A. Goddard, *Science* **239**, 896 (1988).
 - 43 Y. Tokura, J. B. Torrance, T. C. Huang, and A. Nazzal, *Phys. Rev. B* **38**, 7156 (1988).
 - 44 R. C. Karnatak, J. M. Esteva, H. Dexpert, M. Gasgnier, P. E. Caro, and L. Albert, *J. Magn. Magn. Mater.* **63–64**, 518 (1987).
 - 45 A. K. McMahan and R. M. Martin, in *Narrow Band Phenomena*, edited by J. C. Fuggle, G. A. Sawatzky, and J. W. Allen (Plenum, New York, 1988), p. 133.
 - 46 S. Chittipeddi, Y. Song, J. P. Golben, D. L. Cox, J. R. Gaines, and A. J. Epstein, *Phys. Rev. B* **37**, 7454 (1988).
 - 47 P. W. Anderson, *Phys. Rev.* **124**, 41 (1961).
 - 48 C. M. Varma, *Rev. Mod. Phys.* **48**, 219 (1976).
 - 49 J. M. Lawrence, P. S. Riseborough and R. D. Parks, *Rep. Prog. Phys.* **44**, 1 (1981).
 - 50 F. C. Zhang and T. M. Rice, *Phys. Rev. B* **37**, 3759 (1988).
 - 51 We should point out that Eqs. (5.1)–(5.4) potentially explain the drastically reduced transition temperature found in $\text{YBa}_2\text{Cu}_2\text{O}_{7-y}$ doped with small amounts of Zn where instead of Pr $4f$ levels near E_F , we have the filled Zn $3d$ shell. See C.-S. Jee, D. Nichols, A. Kebede, S. Rahman, J. E. Crow, A.

- M. Ponte-Goncalves, T. Mihalisin, G. H. Myer, I. Perez, R. E. Salomon, P. Schlottmann, S. H. Bloom, M. V. Kuric, Y. S. Yao, and R. P. Guertin, *J. Supercon.* **1**, 63 (1988).
- ⁵²A. P. Gonçalves, I. C. Santos, E. B. Lopes, R. T. Henriques, and M. Almeida (unpublished).
- ⁵³A. Kebede, C. S. Jee, J. Schwegler, J. E. Crow, T. Mihalisin, G. H. Myer, R. E. Salomon, P. Schlottmann, M. V. Kuric, S. H. Bloom, and R. P. Guertin, *Phys. Rev. B* **40**, 4453 (1989).
- ⁵⁴M. F. Hundley, J. D. Thompson, S-W. Cheong, Z. Fis, and S. B. Oseroff, *Physica* **158C**, 102 (1989).
- ⁵⁵R. B. Beyers, B. T. Ahn, G. Gorman, V. Y. Lee, S. S. P. Parkin, M. L. Ramirez, K. P. Roche, J. E. Vazquez, T. M. Gür, and R. A. Huggins, *Nature* **340**, 619 (1989).
- ⁵⁶A. P. Gonçalves, I. C. Santos, E. B. Lopes, R. T. Henriques, M. Almeida, and L. Alcacer, *Proceedings of the IX Winter Meeting in Low Temperature Physics: High Temperature Superconductors, Vista Hermoso, Mexico, 1988*, edited by J. Heiras (World Scientific, Singapore, 1988), p. 256.
- ⁵⁷A. P. Gonçalves, I. C. Santos, E. B. Lopes, R. T. Henriques, M. Almeida, O. Figueiredo, J. H. Alves, and M. Godinho, *Physica C* **153-155**, 910 (1988).
- ⁵⁸P. M. Chaikin and G. Beni, *Phys. Rev. B* **13**, 647 (1976).
- ⁵⁹I. Zoric and R. D. Parks, in *Valence Instabilities and Related Narrow-Band Phenomena*, edited by R. D. Parks (Plenum, New York, 1977), p. 459.
- ⁶⁰M. E. López-Morales, R. J. Savoy, and P. M. Grant, *Solid State Commun.* **71**, 1079 (1989).